Heat transport in nano materials subject to high intensity nano focused X-rays

Harald Wallander

Thesis submitted for the degree of Bachelor of Science
Project duration: 2 months

Supervised by J. Wallentin

LUND
UNIVERSITY

Department of Physics
Division of synchrotron radiation physics
June 2016

Abstract

The thesis aims to investigate the amount and distribution of heat in nano materials irradiated by highly focused X-ray beams, like those that will be produced by MAX IV. The beam used in the study had a flux of 10^{11} photons per second and a diameter of 100 nm. The materials studied were a 2 µm long and 100 nm wide Indium phosphide (InP) nanowire on a Silicon nitride (Si_3N_4) substrate, a similar 3 µm long nanowire with gold contacts and a gold drop on a silicon substrate. COMSOL, utilising the Finite element method (FEM), was used to calculate the temperatures. The temperatures of the sample varied between 20 °C and 25 °C in most cases, except for high photon fluxes when it reached 90 °C. The room temperature was set to 20 °C. The materials reached steady state in the order of a few to a few tens of nanoseconds. The conductance of heat between the sample and the substrate was found to be the most significant factor affecting the maximum temperature reached by the sample. Radiative heat loss does not seem to be significant for the conditions studied.

Contents

Acronyms

FEM Finite element method. 3, 1, 7, 8

FWHM Full width half maximum. 6, 8, 15

InP Indium phosphide. 3, 5, 6, 8, 9, 11, 12, 13, 14, 15, 17

Si_3N_4 Silicon nitride. 3, 5, 6, 8, 9

1 Introduction

During X-ray radiation experiments there exists the possibility of the sample being damaged by the radiation. One of these damaging effects is the heating of the sample irradiated by the X-rays. While both the absorption of electromagnetic radiation in matter and the transport of heat are well understood the temperatures reached by the sample depends on its geometry as well as on material properties. Therefore determining the temperature of the sample is not always as simple as understanding the underlying principles of heat absorption and heat transfer. This work seeks to investigate the characteristics of this heating for a set of common beam targets using FEM. To implement the final element method a software package called COMSOL was used. The work will determine how different factors such as beam power and diameter, conductance between sample and substrate or sample size will affect the temperatures reached by the sample. This is a theoretical work and do not include original experimental data.

1.1 Synchrotron radiation research

Synchrotron radiation research has benefited many areas or science. The fields where it has had the biggest impact are material science, nanoscience, life science, biology, chemistry and environmental sciences. The reason synchrotron radiation has proven so useful in these fields is that it produces X-rays, which have wavelengths in the order of nanometres. This is the same order of magnitude as the smallest building blocks in both material science and biological systems which allows diffraction experiments to be carried out to study crystal structures, surface chemistry, proteins, cells, chemical reactions etc.

Further, by focusing the beam down to a few tens of nanometres more detailed results can be obtained. The new NanoMAX beam line at the MAX IV laboratory will do exactly this (a schematic view can be seen in fig 1). This beam line will have a photon energy range of 5 to 30 keV and a raw flux from the undulator of about 10^{15} photons per second, although the flux after passing through all the optics will be considerably lower[1] at about 10^{10}. The power of the beam at 10^{10} photons per second is in the order of µW. The focus of the beam is expected to be 30 to 50nm with a goal of 10 nm[1].

With NanoMAX it will be possible to make local measurements on the nano scale, rather than examining a large part of the sample at once. For example it will be possible to image the internal structure of materials on the atomic scale, determining arrangement and localising defects. By determining the lattice constant of materials locally the internal strains and stresses can be determined. Thanks

to a high flux (photons per second) it will also be possible to continuously image systems as they evolve in time[2].

This last possibility of being able to obtain highly time resolved X-ray images will have great applications in studying the production processes of many different materials, determining the strain and chemistry of the materials at different stages of their formation. Examples are catalysts and components of solar cells (which are often in the nano scale) and the formation of alloys.

The higher the energy of the radiation is, the deeper it will penetrate into the sample. It is thanks to the MAX IV will have the ability to produce high energy X-rays (hard X-rays) that it will be possible to image processes taking place deep inside materials or machines. This is done without destroying them, much like an X-ray in a hospital can reveal the structure of the skeleton without damaging surrounding tissue.

An example of a type of experiment that is done using the radiation absorbed in the sample is X-ray fluorescence experiments. Here the electron vacancy left in the atom that absorbed the X-ray will be filled by other nearby electrons emitting photons of wavelengths characteristic of the element in the process. It is often used in life science, for example to determine the amount of pollutants or trace elements in a sample, such as in ref[3].

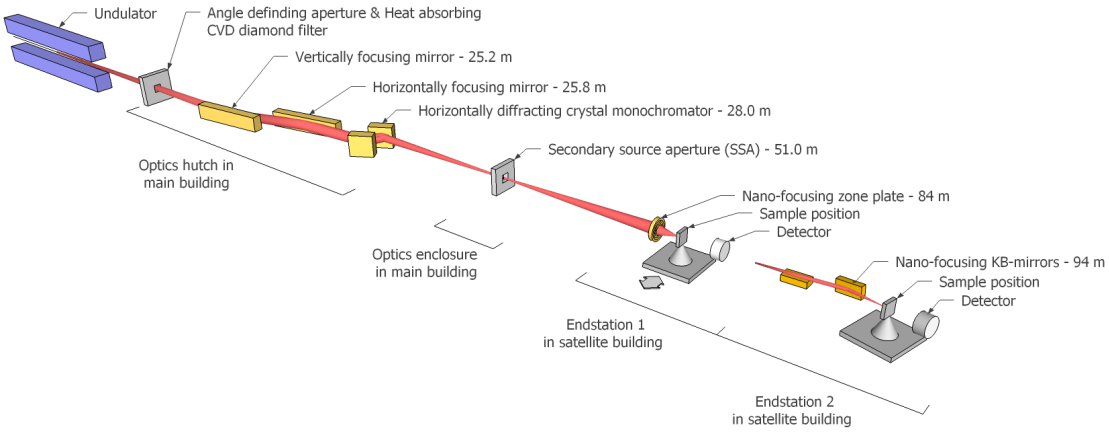

Figure 1: *An overview of the new nanoMAX beam line at the MAX IV laboratory[2]. Here the X-ray beam will be able to be focused down to a few tens of nanometres in diameter.*

Current research involving synchrotron radiation includes the study of using nanowires as X-ray detectors themselves, such as in ref[4]. Here a horizontal InP nanowire with gold contacts at the ends is used as a pixel in an X-ray detector. By doing this the authors reached the highest resolution possible by decreasing the pixel size of the detector. The situation is very similar to the experiments that will take place at NanoMAX.

In another experiment, using an X-ray laser, cells were imaged[5]. The article mentions that sub nanometre resolution would be achievable, but that the pulsing of the laser and the X-ray detectors need improvement. The latter could possibly be resolved with the help of the results from the previous article.

1.2 X-ray interaction with matter

When passing through matter some X-rays will scatter, either elastically (Thomson scattering) or inelastically (Compton scattering), and in most research it is this scattered radiation that is used for experiments. Some X-rays will undergo photoelectric absorption. That is when a photon transfers all of its energy to an atom in a material and ionises it. Depending on the thickness of the sample, energy of the X-rays and the materials in the target many (usually most) of the X-rays may also simply pass through the sample.

The photoelectric effect is the most important effect to consider when studying the energy absorption in a material subject to radiation. The absorption coefficient for the resulting electron is much shorter than that for an X-ray and will deposit all its energy very locally.
The number of these absorption events that take place per time determines how much power will be transferred to the material. How many ionisation events will take place per unit time in turn depends on the number of photons in the beam per unit time and how well the elements in the material absorb X-rays. With each absorption event the intensity of the beam will decrease and it is possible to calculate the number of absorptions by describing the change in intensity as the beam passes through the material.
The intensity of the beam inside the material is given by $I(z) = I_0 \cdot e^{-\mu z}$ where I is the intensity, I_0 is the original intensity, z is the depth and μ is the absorption coefficient. The absorbed radiation is simply calculated as the difference between the initial and the transmitted intensities: $I_{absorbed} = I_0 - I_z$.

The absorption coefficient depends on the density of the material and the atomic absorption cross section, σ_a: $\mu = \rho_{at} \cdot \sigma_a$, which is in turn determined by $\sigma_a = 2 \cdot r_e \cdot \lambda \cdot f_2$ where r_e is the Lorentz radius (or classical electron radius), λ is the wavelength of the light and f_2 is the imaginary part of the complex atomic scattering factor[6;7]. This part of the scattering factor, f_2, is itself strongly dependent on the wavelength of the light and is related to how well the energy of the X-rays match the energies of the electrons in its different shells. At the CXRO[8] web site values for f_2 are tabulated for a range of different elements and X-ray energies.

1.3 Heat transport

The differential equation for heat transfer is $k \cdot \nabla^2 T + q_0 = 0$ where k is the thermal conductivity, T is the temperature, ∇^2 is the Laplace operator and q_0 is the internal heat source[9]. To solve it one first needs to know the thermal conductivity of all materials involved. This is a tabulated value that can be found at, for example, sites such as ref[10] and ref[11]. One also need to know the flow of heat into and out of the system. The influx is calculated using the absorption coefficient in the previous section. To calculate the outflow of heat one needs to know the emissivity, ε , of the materials involved (can be found at ref[11] and ref[12]), the ambient temperature, the convective elements of heat transfer and any boundary conditions. The convective terms are determined by the geometry and could be handled within COMSOL. The ambient temperature and boundary conditions can be chosen arbitrarily and is typically set to room temperature (20 °C).

The radiative loss of heat from the sample is governed by the Stefan-Boltzmann law: $e_b(T) = \sigma T^4$ where σ is the Boltzmann constant and T is the absolute temperature. The sample also receives heat radiated from the ambience, governed by the same law. The law holds true for a black body radiator, which is not accurate for most materials as they are not perfect black body radiators. This fact is accounted for by the emissivity, ε , of the material. The emissivity is material and wavelength dependent. The net flow of heat between sample and ambiance, Q, due to radiation is: $Q = A \cdot F_{1-2} \cdot \sigma(T_1^4 - T_2^4)$ where Q is the flow of heat, A is the area, F is the configuration factor (related to the surface shape and emissivity of the material) and T_1 and T_2 are the temperatures of the two radiating bodies.

The final piece of solving the heat transfer problem is to estimate the thermal conductance between the different materials, called contact resistance or gap conductance $h_c[\frac{W}{m^2K}]$. It is defined similarly to a heat transfer coefficient and can be expressed by: $Q = h_c \cdot A \cdot \Delta T$ where Q is the heat flowing across the interface, A is the area of the surfaces, ΔT is the temperature difference over the interface and

h_c is the gap conductance[9]. Including gap conductance results in a more complex problem as it depends on the phonon frequencies of the different materials and the proportion of the materials that are in direct contact. Typically materials do not have the same phonon frequencies (which creates a thermal resistance across the interface) and due to roughness of the surfaces only part of the two surfaces are in direct contact with each other (on the atomic level) which further decreases the amount of heat that will flow across this interface. The effect of the phonon frequency mismatch can be calculated but the contact area is harder to determine and could also vary considerably from case to case. Often one has to rely on empirical values for the contact resistance.

1.4 Motivation

When diffraction experiments are carried out some of the X-rays used will absorb in the sample instead of being reflected of pass through. These absorbed X-rays heat up the sample which can damage it or interfere with measurements. The purpose of this work is to investigate how big the heating is in different materials and what the main factors influencing the temperature are.

Especially with the opening of the MAX IV laboratory and the NanoMAX beam line the effect of a highly focused X-ray beam on materials will be of interest. What will be studied is how different parameters affect the temperature reached by the sample, how local the distribution of the heat is and how quickly the samples heat up and cool down again. This last aspect will be of interest during the experiments using a scanning X-ray beam.

2 System studied

During the project several systems were simulated and many variables were varied. To reduce the number of combinations one reference system was used and variables changed individually in relation to this reference system. The reference system used here is that of a 100 nm wide 2 µm long hexagonal InP nanowire lying on a substrate of Si_3N_4. The nanowire also has a gold droplet attached to one of its ends. This is a remnant from the fabrication process. Two special cases were also studied; a modified system where two gold contacts had been added to a similar but 3 µm long nanowire and a system with a gold drop on a Si substrate. All systems are shown in figure 2.

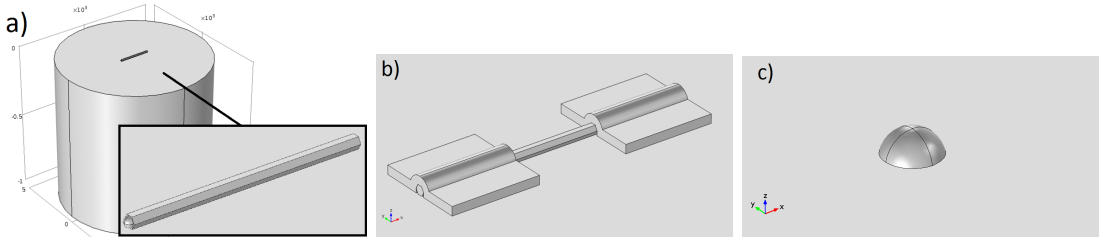

Figure 2: *a) A* 2 µm *InP nanowire on a* Si_3N_4 *substrate. The inset is a detail of the nanowire. b) a* 3 µm *InP nanowire on a* Si_3N_4 *substrate with added gold contacts. Substrate shape is the same as in the picture on the left. c) Gold drops on a Si substrate. Substrate shape is the same as in the picture on the left.*

The samples above were simulated to be subject to an X-ray beam with a Gaussian distribution with a variance of $\sigma = 50\,\text{nm}$, equivalent to a beam with a diameter of 100 nm (can be seen in figure 3). In the reference system the beam hit the wire in the middle at a 90° angle. The beam was assumed to consist of 10 keV photons and have a flux of 10^{11} photons per second. The resulting beam power is 160 µW. The absorption coefficients for the different materials used was calculated using the equations given in the introduction. Using these relations the absorption coefficients for InP, Si_3N_4, Au and Si were calculated to be: $\mu_{InP} = 50\,616\,\text{m}^{-1}$, $\mu_{Si3N4} = 6505\,\text{m}^{-1}$, $\mu_{Au} = 220\,770\,\text{m}^{-1}$ and $\mu_{Si} = 7345\,\text{m}^{-1}$ respectively.

The intensity of the beam decays exponentially as it passes through the sample. However, as the absorption length for X-rays in these materials (4.5 µm for Au - 20 µm for InP) are larger than the size of the system (in the order of a few µm at most) the intensity decays almost linearly. Using these simplifications the calculation of the absorbed power becomes very straightforward. The exponential decay law is simplified as: $I(z) = I_0 \cdot e^{-\mu z} \approx I_0 - I_0\mu \cdot z$ and the absorbed power is calculated by $I(z=0) - I(z) = I_0 - I_0\mu \cdot 0 - (I_0 - I_0\mu \cdot z) = I_0\mu \cdot z$.

The gap conductance between the different materials varied and for the case of the gold contacts and gold drops was taken from[13]. For the (important) case of InP and Si_3N_4 the gap conductance was (fairly arbitrarily) set to 10% of the value for the gold contacts at $8.2\,\text{MW}\,\text{m}^{-1}\,\text{K}^{-2}$. The reason for the lower value is mainly that while the gold contacts and drops are melted onto the substrate (which ought to create a very well connected interface) the InP nanowire had been grown separately and put on the substrate as a solid object. While the surfaces of the substrate and the nanowire are very smooth there are still irregularities. As the gold drop on the tip of the nanowire is in reality slightly wider in diameter than the nanowire (not narrower as in this model) it could also contribute to decreasing the contact between the substrate and the lying nanowire.

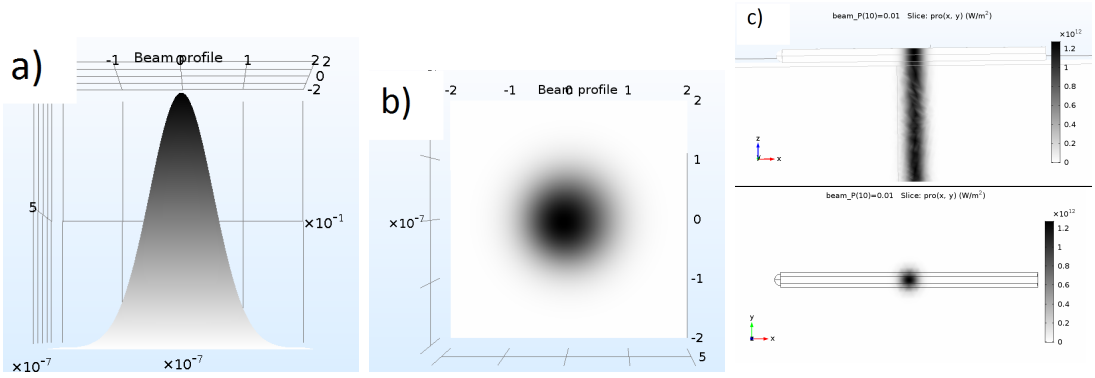

Figure 3: *The beam profile. The beam had a Full width half maximum (FWHM) of* 100 nm *and a power of* 160 µW*. Figures a) and b) show the beam profile from different directions while c) shows where the beam hit the target.*

The modes of heat transfer out of the system were assumed to be limited to convection and radiation to the surrounding environment. After tests the radiation exchange between the nanowire and the substrate was ignored as it did not noticeably change the results but increased computation times considerably.
The variables that were changed were beam power, beam diameter, nanowire diameter and gap conductance between nanowire and substrate. A time dependent simulation were also made displaying the first moments the beam hit the sample and subsequent cooling as the beam was switched off.

3 Algorithms

3.1 Finite element method

The numerical method used in this thesis project is called the FEM. It is a general method used to solve differential equations, in this case the heat equation. The reason the FEM method is used rather than simpler, more common methods such as finite difference methods is that the FEM can easily accommodate complex geometries.

The essence of the FEM is to divide the domain the differential equation is to be solved over into sub-domains.[14] In our case the domain is the geometry of the nanowire and the substrate. The sub-domains are called elements and are created by covering the domain in a mesh of connected lines. The elements are the spaces in between the lines and can be one, two or three dimensional depending on the dimensionality of the domain. Typically, the elements are tetrahedral for a three dimensional mesh. A solution to the differential equation can then be found iter-

atively for each element using given boundary conditions. An example of one of the meshes used in this project can be seen in figure 4.

The way the values are calculated within each element is by using the weighted residual method; one assumes a trial function defined only within an element and then fit that trial function as closely as possible to the real function. The weighted residual method is used in its weak form to enable simpler trial functions to be used. The value of the differential equation within an element is then constant, instead the value at the element edges, the nodes, approaches the true value of the differential equation.

The boundary conditions are given for certain nodes in the domain. The value in the boundary node will then affect the value calculated for the other nodes connected to the same element. Those nodes will in turn affect adjacent elements and a solution for the whole domain can be found iteratively. It is the division of the domain into simpler elements that makes the FEM method able to deal with complex geometries.

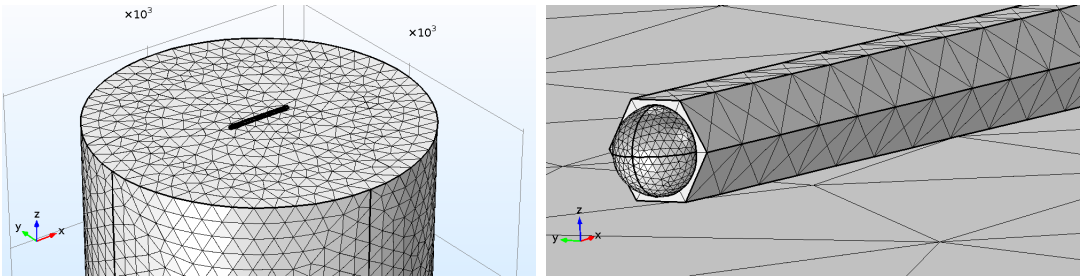

Figure 4: *Left: The mesh created for the single InP nanowire on substrate system Right: A detail from the same mesh. Here only the surface of the mesh is seen, the real mesh is three dimensional and consists of tetrahedra.*

3.2 COMSOL

As the implementation of the FEM is rather intricate and building meshes is an advanced topic COMSOL[15] was used for all simulations in this project. COMSOL is a software package for solving physics problems that utilises the FEM. It also includes a CAD kernel for building the geometries of the systems studied.

4 Results

The steady state temperature distribution was calculated for the reference system with a 2 µm long, 100 nm wide InP nanowire on a cylindrical substrate of Si_3N_4 with height 10 µm and radius 5 µm. The reference system also had a beam flux of 10^{11} 10 keV photons per second (or a beam power of 160 µW), a beam diameter of 100 nm (at FWHM of the Gaussian beam profile) and a gap conductance between nanowire and substrate of 8.2 $\frac{MW}{m^2 \cdot K}$. The ambient temperature and the original temperature of the sample were both set to 20 °C.
Values for the thermal conductivity (k), heat capacity at constant pressure (c_p) and emissivity (ε) for the different materials are given in table 1.

The values for the beam power, beam diameter, nanowire diameter and gap conductance were varied independently with the reference system as a basis. Lastly the time dependent heating was plotted for all three systems; the InP nanowire, nanowire with contacts and gold drops on a Si substrate. The time dependent simulations used the reference values in all cases with the exception that the beam power was set to 0 W after the system reached stable temperature.

Table 1: **Material properties used in simulations**

	k ($W\,m^{-1}\,K^{-1}$)	c_p ($J\,kg^{-1}\,K^{-1}$)	ε
InP	68	310	0.695
Si_3N_4	27	711	0.67
Si	130	700	0.67
Au	318	126	0.47

4.1 InP nanowire on substrate

Temperature of the InP nanowire as a function of beam power 1

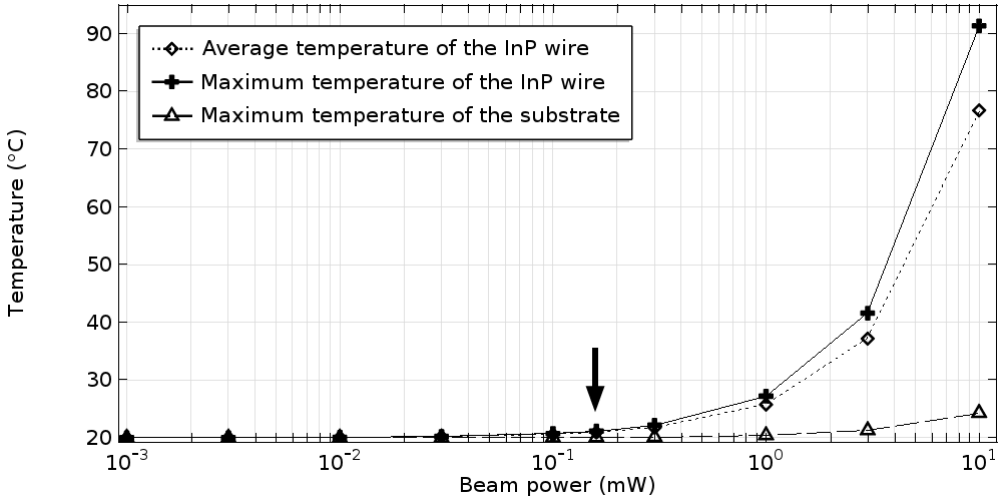

Figure 5: *The temperature of the nanowire is plotted against beam power. The dotted line shows the average temperature of the InP nanowire, the solid line shows the maximum temperature of the InP nanowire and the dashed line shows the maximum temperature of the substrate. The markers show the data points used in the simulation. The simulation was run for beam powers of* 1 µW, 3 µW, 10 µW, 30 µW, 100 µW, 160 µW, 300 µW, 1 mW, 3 mW *and* 10 mW. *The gap conductance was* 8.2 MW m^{-1} K^{-2}, *the beam diameter was* 100 nm *and the nanowire diameter was* 100 nm.

Temperature of the InP nanowire as a function of beam power 2

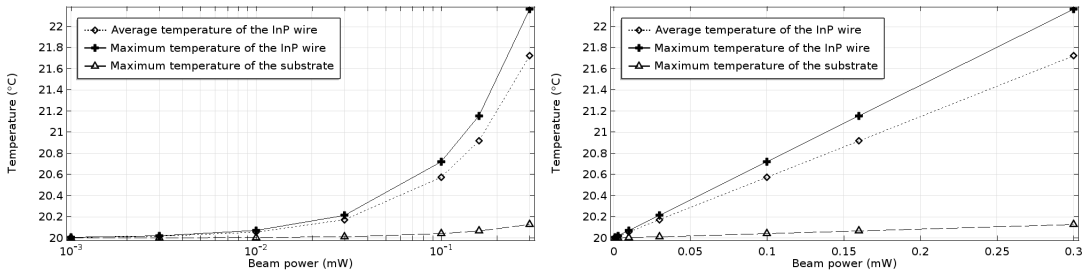

Figure 6: *This is the lower range of values in figure 5, the maximum power solved for is* 300 µW. *Left is a logarithmic plot of the 0.1 - 300* µW *range and right is a linear plot.*

In the beam power plot (figure 5) the temperature increase is linear, or proportional to the amount of energy flowing into the target. As the temperature difference between the target and the surroundings increases the effect of radiative loss from target to the surroundings should also increase. As more heat is lost as radiation at higher temperatures one might expect the beam power to have a diminished effect on sample temperature at high fluxes. However, this does not appear to be the case. This could indicate that radiative loss does not significantly contribute to the heat loss of the nanowire, even at relatively high temperatures.

Temperature of the InP nanowire as a function of gap conductance

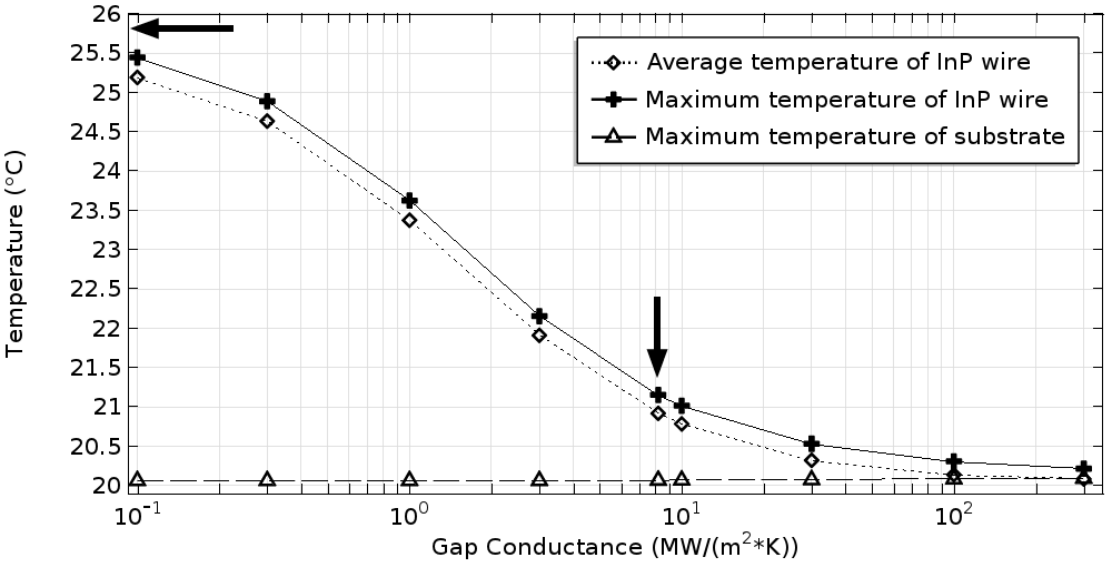

Figure 7: *The temperature of the nanowire is plotted against gap conductance between the nanowire and the substrate. The dotted line shows the average temperature of the InP nanowire, the solid line shows the maximum temperature of the InP nanowire and the dashed line shows the maximum temperature of the substrate. The markers show the data points used in the simulation. The simulation was run for gap conductances of 0.1, 0.3, 1, 3, 8.2, 10, 30, 100 and 300* $\mathrm{MW\,m^{-1}\,K^{-2}}$. *The beam power was* 160 µW*, the beam diameter was* 100 nm *and the nanowire diameter was* 100 nm.

The temperature for a gap conductance of $0\,\mathrm{MW\,m^{-1}\,K^{-2}}$ was also calculated, but cannot be shown in the logarithmic plot above. The maximum temperature of the InP nanowire for 0 gap conductance was $T_{max} = 28.8\,°C$, the average $T_{av} = 25.5\,°C$ and the maximum substrate temperature was $T_{sub} = 20.1\,°C$.

Gap conductance had a strong effect on sample temperature (figure 7). This suggests that gap conductance is the primary source of heat loss in the nanowire. The true (or typical) value for the gap conductance is not really known for the system studied. It could also vary considerably. Factors that would affect the gap conductance are impurities on the surfaces of nanowire or substrate, load on the nanowire or Van der Waals forces between nanowire and substrate. The geometry of the materials also affects the gap conductance. For example, in many cases the gold droplet used to grow the nanowire is often slightly wider than the nanowire diameter (rather than smaller, as in this simulation) which would partially lift the nanowire off the substrate. Not all nanowires are hexagonal or have flat walls. Some have a more corrugated surface or might be circular in cross section. Such wires would have much poorer contact with the substrate than the wires studied in this simulation.

Temperature distribution of the InP nanowire for a gap conductance of $300\,\mathrm{MW\,m^{-1}\,K^{-2}}$

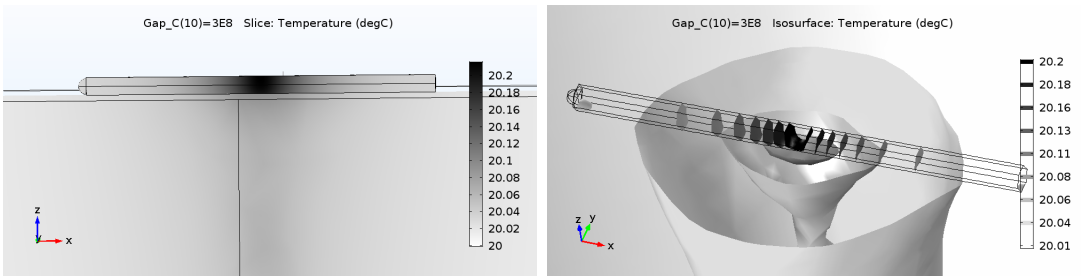

Figure 8: *The temperature distribution inside the nanowire. Left: a cross section of the temperature inside the target. Right: isothermal contours inside the target. The beam power was* $160\,\mu\mathrm{W}$*, the gap conductance was* $300\,\mathrm{MW\,m^{-1}\,K^{-2}}$*, the beam diameter was* $100\,\mathrm{nm}$ *and the nanowire diameter was* $100\,\mathrm{nm}$*.*

Temperature of the InP nanowire as a function of beam diameter

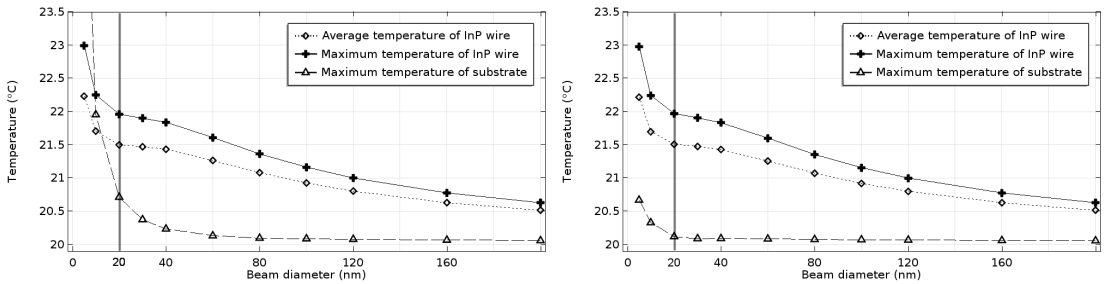

Figure 9: *The temperature of the nanowire is plotted against beam diameter. The low diameter results are non-physical. Two plots are made; left: larger mesh size of the substrate, right: smaller mesh size of the substrate. The dotted lines show the average temperature of the InP nanowire, the solid lines show the maximum temperature of the InP nanowire and the dashed lines show the maximum temperature of the substrate. The markers show the data points used in the simulation. The simulation was run for beam diameters of* 5 nm, 10 nm, 20 nm, 30 nm, 40 nm, 60 nm, 80 nm, 100 nm, 120 nm, 160 nm, *and* 200 nm. *The beam power was* 160 µW, *the gap conductance was* 8.2 MW m^{-1} K^{-2} *and the nanowire diameter was* 100 nm.

The results for the beam diameter plot are at first rather surprising. While the temperature stabilises at around 40 nm (when the beam wholly hits the nanowire) below 20 nm the temperature increases quickly. The two different plots in figure 9 have different mesh sizes for the substrate. It can be seen that in the first plot (with the larger mesh size) the effect is aggravated for the temperature of the substrate. This indicates that COMSOL fails to determine the temperature accurately if the mesh size is too large compared to the beam diameter.
This is a good example for evaluating the accuracy of the results. This project has been only simulations and is limited by the limitations of the method and assumptions made. Mesh size is clearly an important factor when using the FEM method.

Temperature of the InP nanowire as a function of nanowire diameter

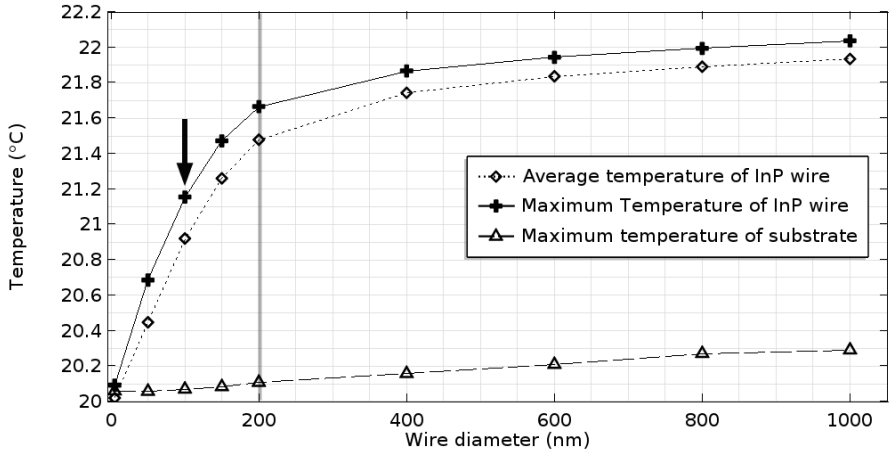

Figure 10: *The temperature of the nanowire is plotted against nanowire diameter. The dotted line shows the average temperature of the InP nanowire, the solid line shows the maximum temperature of the InP nanowire and the dashed line shows the maximum temperature of the substrate. The markers show the data points used in the simulation. The simulation was run for nanowire diameters of* 5 nm, 50 nm, 100 nm, 150 nm, 200 nm, 400 nm, 600 nm, 800 nm *and* 1 µm. *The beam power was* 160 µW, *the gap conductance was* 8.2 MW m^{-1} K^{-2} *and the beam diameter was* 100 nm.

In the plot for nanowire diameter the temperature increases quickly with diameter and then pans out. The power absorbed in the nanowire increases linearly with its diameter but the surface and contact area increases quicker than only with the diameter. It is therefore not surprising that the out flux of heat catches up with the increased influx.

Temperature of the InP nanowire as a function of time

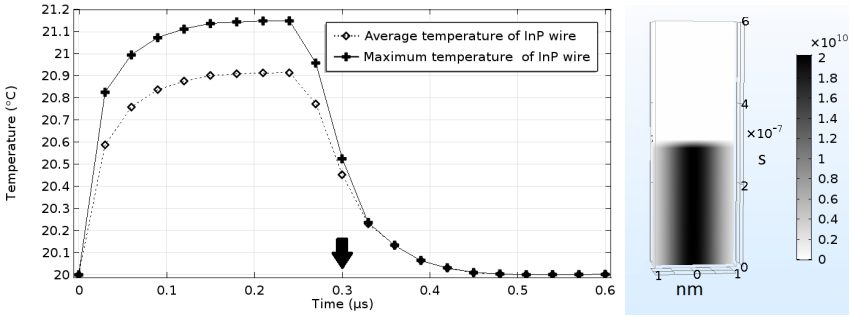

Figure 11: *Left: The temperature of the nanowire is plotted against beam exposure time. The dotted line shows the average temperature of the InP nanowire and the solid line shows the maximum temperature of the InP nanowire. The markers show the data points used in the simulation. The arrow shows where the beam was switched off. Right: The intensity of the beam as a function of radius and time. The beam was switched on at* $t = 0\,\mu s$ *and switched of at* $t = 0.3\,\mu s$ *. The simulation was run for* $0.6\,\mu s$ *with temperatures calculated every* $30\,ns$*. The beam power was* $160\,\mu W$*, the gap conductance was* $8.2\,MW\,m^{-1}\,K^{-2}$*, the beam diameter was* $100\,nm$ *and the nanowire diameter was* $100\,nm$*.*

4.2 InP nanowire with gold contacts

Beam characteristics of the nanowire with gold contacts simulation

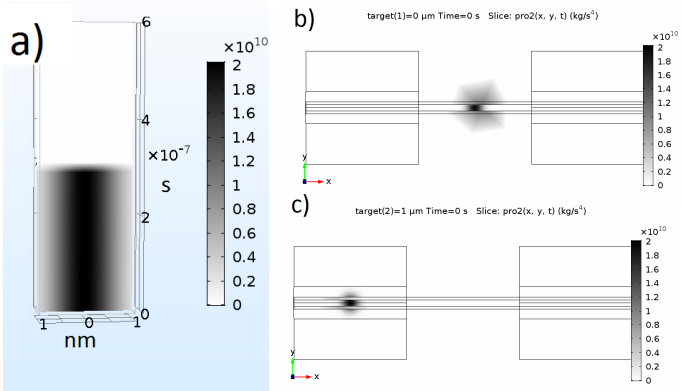

Figure 12: *a) the beam profile as a function of radius and time. b) the target area of the first simulation (to the left in figure 13). c) the target area of the second simulation (to the right in figure 13). The beam had a FWHM of* $100\,nm$ *and a power of* $160\,\mu W$*.*

Temperature of the InP nanowire and gold contacts as a function of time

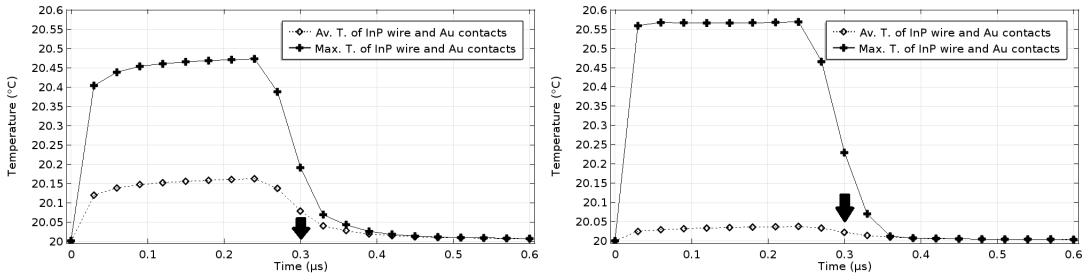

Figure 13: *The temperature of the nanowire and gold contacts is plotted against beam exposure time. The dotted line shows the average temperature of the InP nanowire and Au contacts, the solid line shows the maximum temperature of the InP nanowire and Au contacts. The markers show the data points used in the simulation. The arrow shows where the beam was switched off. Left: the beam hits the target on the nanowire as shown in figure 12 a), right: The beam hits the target on the Au contact as shown in figure 12 b). The simulation was run for* 0.6 µs *with temperatures calculated every* 30 ns*. The beam power was* 160 µW*, the gap conductance was* 8.2 MW m^{-1} K^{-2} *for the nanowire and* 82 MW m^{-1} K^{-2} *for the Au contacts, the beam diameter was* 100 nm *and the nanowire diameter was* 100 nm*.*

The time dependent plots (figures 11, 13 and 14) show a very fast increase in temperature. The subsequent cooling is also rapid. Using a diffusive treatment of heat transfer this could possibly be explained by the short distances the heat needs to travel to reach the substrate. A source of error is that the beam did not seem turn off immediately. The cooling starts roughly 50 ns earlier than the 0.3 µs mark when the beam should be switched off. Especially in figures 13 and 14 the cooling seems rather linear and slower than the heating. This happened despite using the square pule in COMSOL which should only have values of 0 and 1.

When the beam hits the gold contact in figure 13 the maximum temperature is higher and the average temperature is lower than the case where the beam hits the wire. As the wire is thin and does not conduct heat as well as the gold most of the heat stays in the contact if the beam hits it. If the beam hits the wire the heat is more evenly distributed in the system and between the contacts leading to a lower maximum temperature and higher average temperature.

4.3 Gold drop on Si substrate

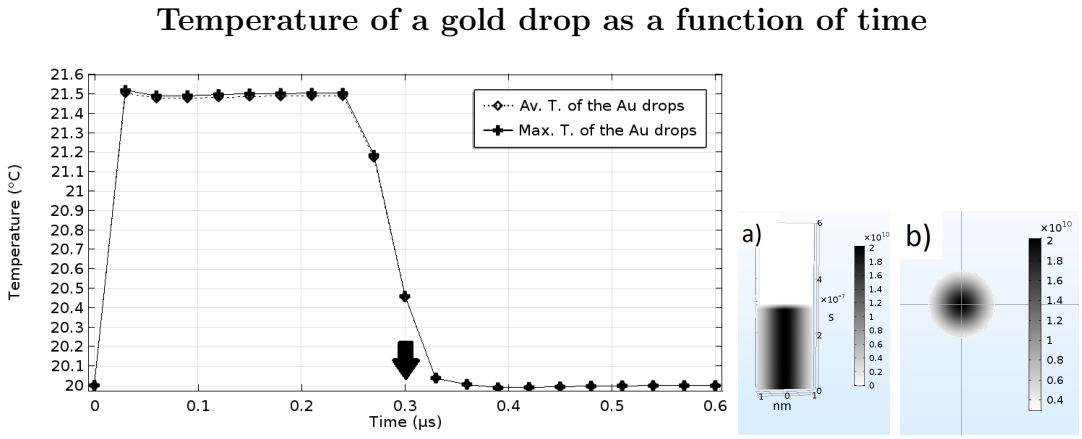

Figure 14: Left: the temperature of the gold drop on a Si substrate is plotted against beam exposure time. The beam hit the gold drop. The dotted line shows the average temperature of the Au drop and the solid line shows the maximum temperature of the Au drop. The markers show the data points used in the simulation. The arrow shows where the beam was switched off. Right: a) the beam profile as a function of radius and time. b) the target are of the beam. The simulation was run for 0.6 µs with temperatures calculated every 30 ns. The beam power was 160 µW, the gap conductance was 82 MW m^{-1} K^{-2}, the beam diameter was 100 nm and the drop diameter was 100 nm.

The maximum temperature in the gold contacts nanowire system (figure 13) was lower than for the lone nanowire. While the gold contact has a higher absorption coefficient than the InP nanowire it also has much better contact with the substrate (in the case simulated here). This is likely the reason why it heats up less than the nanowire for similar circumstances. When the beam hit the gold contact directly the sample heated up much quicker. This is likely due to the higher thermal conductivity and gap conductance of gold compared to InP. The gold drop heated up very quickly and reached the highest temperature of the three time dependent studies. As the gold drop was almost completely covered by the beam this is reasonable. The value used for the gap conductance between gold and the substrate was taken from an experiment with a different substrate, it might not be accurate for the circumstances simulated here.

In most cases the temperature was quite even and the difference between the average and the maximum temperature was not very large. Especially for the smaller systems. The spreading of heat is governed by the same equations governing diffusion, which, as we know, acts very quickly over small distances. This is probably also the reason the gap conductance has such an important role in dissipating the heat absorbed in the nanowire.

5 Outlook

For improving the FEM approach a good idea could have been to purposefully build the mesh so that nodes would be placed in the target area of the beam. It would have allowed a larger mesh to be used for the substrate while still guaranteeing that it heated properly.
Far from all nanowires are hexagonal or have flat sides. Many are round or have corrugated sides. The behaviour of these nanowires would be quite different from the one studied here. Most importantly they would likely have much poorer contact with the substrate and lower gap conductance as a consequence.

The pulsed nature of the light source could have been accounted for as well as the local nature of the absorption. The absorption in each pulse is also random, which could have been interesting to model.
Electrical effects could perhaps have been modelled (especially if one wants to study possible damaging effects that do not directly depend on heating).
A theoretical approach could have been taken to evaluate the gap conductance. Phonon frequencies could have been considered for the theoretical maximum gap conductance. A more detailed evaluation of the contact area could have been made using for example levels of surface roughness of the substrate and the wire.

Apart from the improvements mentioned above it would have been interest to simulate the absorption of X-rays in a cell as many recent experiments have been carried out by putting cells in x-ray beams. To do this one would have to accurately build the geometry of the cell and evaluate its composition and factor in all the absorption coefficients.

References

[1] Ulf Johansson, Ulrich Vogt, and Anders Mikkelsen. Nanomax: a hard x-ray nanoprobe beamline at max iv, 2013.

[2] MAX IV laboratry nanomax. https://www.maxlab.lu.se. Accessed: 2016-04-22.

[3] S. Bamford, D. Wegrzynek, E. Chinea-Cano, et al. Application of x-ray fluorescence techniques for the determination of hazardous and essential trace elements in environmental and biological materials. *Nukleonika*, 49(3):87–95, 2004.

[4] Jesper Wallentin, Markus Osterhoff, Robin N. Wilke, et al. Hard X-ray Detection Using a Single nm Diameter Nanowire. *NANO LETTERS*, 14(12):7071–7076, DEC 2014.

[5] Gijs van der Schot, Martin Svenda, Filipe R. N. C. Maia, et al. Imaging single cells in a beam of live cyanobacteria with an X-ray laser. *Nature Communications*, 6, FEB 2015.

[6] Jens Als-Nielsen and Des McMorrow. *X-rays and their interaction with matter*. John Wiley & Sons, Inc., second edition, 2011.

[7] Albert C. Thompson, David T. Attwood, Eric M. Gullikson, et al. X-ray data booklet, 2001.

[8] CXRO optical constants. http://henke.lbl.gov/optical_constants/asf.html. Accessed: 2016-04-12.

[9] John H. Lienhard IV and John H. Lienhard V. *X-rays and their interaction with matter*. Phlogiston Press, fourth edition, 2011.

[10] IOFFE thermal constants. http://www.ioffe.ru/SVA/NSM/Semicond/l. Accessed: 2016-04-25.

[11] K-Space thermal constants. http://www.k-space.com/support/material-properties/l. Accessed: 2016-04-25.

[12] CeramicIndustry thermal constants. https://www.ceramicindustry.com/ext/resources/pdfs/2013-CCD-Material-Charts.pdf. Accessed: 2016-04-25.

[13] Takafumi Oyake, Masanori Sakata, and Junichiro Shiomi. Nanoscale thermal conductivity spectroscopy by using gold nano-islands heat absorbers. *Applied Physics Letters*, 106(7), 2015.

[14] P. Seshu. *Textbook of Finite Element Analysis*. PHI Learning Private Limited, 2003.

[15] COMSOL multiphysics. https://www.comsol.se/. Accessed: 2016-05-02.